

Laser cooling with electromagnetically induced transparency: Application to trapped samples of ions or neutral atoms

F. Schmidt-Kaler, J. Eschner, G. Morigi⁽¹⁾, C. F. Roos⁺, D. Leibfried*, A. Mundt, R. Blatt
Institut für Experimentalphysik, University of Innsbruck, A-6020 Innsbruck, Austria
⁽¹⁾*Max-Planck-Institut für Quantenoptik, D-85748 Garching, Germany*

A novel method of ground state laser cooling of trapped atoms utilizes the absorption profile of a three (or multi-) level system which is tailored by a quantum interference. With cooling rates comparable to conventional sideband cooling, lower final temperatures may be achieved. The method was experimentally implemented to cool a single Ca^+ ion to its vibrational ground state. Since a broad band of vibrational frequencies can be cooled simultaneously, the technique will be particularly useful for the cooling of larger ion strings, thereby being of great practical importance for initializing a quantum register based on trapped ions. We also discuss its application to different level schemes and for ground state cooling of neutral atoms trapped by a far detuned standing wave laser field.

PACS:

I. INTRODUCTION

The emergence of schemes that utilize trapped ions or atoms for quantum information, and the interest in quantum statistics of ultra cold atoms, have provided renewed interest for laser cooling techniques. Starting with the case of a single atom, the present goal is now to laser cool larger numbers of atoms and to prepare them for applications e.g. as a quantum register. The cooling of a large number of particles using lasers is a prerequisite for coherent control of atomic systems.

Trapped ions in linear Paul traps are currently considered to be promising candidates for a scalable implementation of quantum computation [1]. Long lived internal states serve to hold the quantum information (qubits) and are manipulated coherently (single-bit gates) by laser beams focused on the ions [2]. The excitation of the ion's common vibrational motion (gate mode) provides the coupling between qubits which is necessary for two-bit quantum gate between ions. The Cirac-Zoller proposal for a two-bit gate [3] requires that initially the gate mode is optically cooled to the ground state. Later Mølmer and Sørensen proposed a two-bit gate which releases this condition and only requires cooling into the Lamb-Dicke regime, typically with a mean vibrational quantum number $\bar{m} \leq 1$ [4,5].

In general, the motion of a string of N cold trapped ions in a linear Paul trap is described by $3N$ harmonic modes of vibration. Cooling *all modes* close to the vibrational ground state is a prerequisite to realizing quantum gates with high fidelity. In typical experimental situations this requires cooling techniques which lead to lower mean vibrational state than simple Doppler cooling. Sideband cooling has been shown to achieve sub-Doppler temperatures [6–9] but proves increasingly inefficient for cooling many modes. The recently proposed method of EIT-cooling provides parallel multi-mode cool-

ing while its experimental effort is significantly reduced.

The first part of this paper (Sec. IIB) describes the principle of the EIT-cooling method and illustrates its results with several realistic examples, the cooling of a single Hg^+ ion held in a Paul trap, and of neutral Rb atoms confined in a far-detuned optical dipole trap (sect. IID). In section III we report the first experimental demonstration of the EIT-method, achieving ground state cooling of a single trapped Ca^+ ion. The detailed description of all necessary experimental ingredients and measurements is meant to provide a recipe for implementing EIT-cooling in various experimental situations. We conclude by a proposal for cooling a linear string of ions (Sec. V), and discuss the relevance for quantum information processing.

II. THE PRINCIPLE OF EIT-COOLING

A. Cooling basics

The theory of laser cooling of atoms in a harmonic trap has been extensively discussed in the literature, see [10] for a comprehensive review. In many experimental situations a simple, intuitive rate equation picture [11] applies which can also be derived from the general theory in the appropriate limits [10]. In this section we recall those intuitive considerations, a detailed theoretical derivation being beyond the scope of this paper.

Consider a trapped 2-level atom with states $|g\rangle$ and $|e\rangle$, excited below saturation by a laser detuned from resonance by Δ . The scattering rate, i.e. steady-state excited state population times decay rate, is denoted by $W(\Delta)$. The atom is coupled to one vibrational degree of freedom, a harmonic oscillator with frequency ν and quantum states $|n\rangle$, such that the internal transition $|g\rangle \leftrightarrow |e\rangle$ splits up into transitions $|g, n\rangle \leftrightarrow |e, n'\rangle$.

The coupling between different motional states is mediated by the recoil of a laser or spontaneous photon. We restrict ourselves to the so-called Lamb-Dicke regime $\eta \equiv k\sqrt{\langle x^2 \rangle} \ll 1$ where the spatial extension of the motional wave packet $\sqrt{\langle x^2 \rangle}$ is smaller than the laser wavelength $\lambda = 2\pi/k$. In this limit the relevant transitions are $|n\rangle \rightarrow |n\rangle$ (carrier) and $|n\rangle \rightarrow |n \pm 1\rangle$ (sidebands). See Fig. 1a for an illustration.

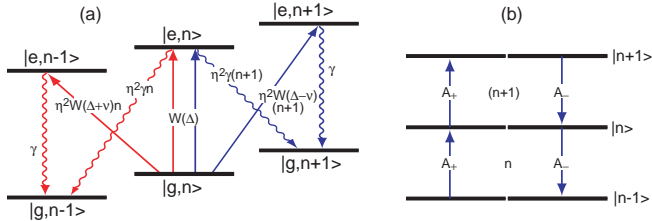


FIG. 1. (a) Cooling ($|n\rangle \rightarrow |n-1\rangle$) and heating ($|n\rangle \rightarrow |n+1\rangle$) transitions starting from state $|g, n\rangle$, at lowest order in η . The relative probabilities of the individual processes are indicated. (b) Illustration of the rate coefficients for cooling and heating, after [10].

The probability that scattering of a photon takes the atom from $|g, n\rangle$ to $|g, n \pm 1\rangle$ has two contributions, corresponding to the two possible intermediate states $|e, n\rangle$ or $|e, n \pm 1\rangle$. The rate coefficients A_{\pm} for cooling and heating transitions (see Fig. 1b) are therefore given by

$$A_{\pm} = \eta^2 (W(\Delta) + W(\Delta \mp \nu)) . \quad (1)$$

Summing up all processes in lowest order η , a rate equation for the populations $p_n(t)$ of the states $|n\rangle$ is obtained which leads to a simple dynamical equation for the mean vibrational excitation $\langle n(t) \rangle = \sum n p_n(t)$,

$$\frac{d}{dt} \langle n \rangle = -(A_- - A_+) \langle n \rangle + A_+ . \quad (2)$$

In the more general case that the laser k vector is at an angle θ to the direction of vibration, and that the spontaneous recoils are spatially distributed with an average projection α on the vibrational axes [12], Eq. (1) changes into

$$A_{\pm} = \eta^2 (\alpha W(\Delta) + \cos^2(\theta) W(\Delta \mp \nu)) . \quad (3)$$

Using Eqs. (2,3), the cooling limit $\bar{m} \equiv \langle n(\infty) \rangle = A_+ / (A_- - A_+)$ and the cooling time constant, $\tau_{cool} = (A_- - A_+)^{-1}$ can be easily evaluated. One finds the well-known cooling limits $\bar{m} \nu \simeq \gamma/2$ for Doppler cooling where $\gamma > \nu$ and $\Delta = -\gamma/2$, and $\bar{m} \ll 1$ for sideband cooling where $\gamma < \nu$ and $\Delta = -\nu$ [10].

It is useful to look at the transitions displayed in Fig. 1a from a different viewpoint: Absorption on one of the sidebands causes a drift of the motional energy while

carrier absorption, being followed by either cooling or heating emission, causes a diffusion of the energy which in average contributes to heating. Therefore for optimum cooling, absorption on the cooling sideband should be maximized while carrier and heating-sideband absorption should be minimized. This leads to the principle of EIT-cooling.

B. EIT-cooling principle

Electromagnetically induced transparency (EIT), like coherent population trapping or "dark resonance", is a manifestation of quantum interference between atomic transition amplitudes. A review can be found in [13]. EIT arises in three- (or multi-) level systems and consists in the cancellation of the absorption on one transition induced by simultaneous coherent driving of another transition. Consider a 3-level atom as shown in Fig. 1, with ground state $|g\rangle$, stable or metastable state $|r\rangle$ and excited state $|e\rangle$. State $|e\rangle$ has linewidth γ and is coupled to $|g\rangle$ and $|r\rangle$ by dipole transitions which are laser-excited. EIT arises when the detunings of the two lasers from state $|e\rangle$ are equal: The system evolves into a coherent superposition of $|g\rangle$ and $|r\rangle$, and light scattering ceases.

In order to use this situation for cooling, the transition $|r\rangle \rightarrow |e\rangle$ is excited by an intense ("coupling") laser ($\Omega_r \sim \gamma$) at detuning Δ_r above resonance. Then the absorption spectrum on the transition $|g\rangle \rightarrow |e\rangle$ seen by the other ("cooling") laser is described by a Fano-like profile [14] which has three characteristic features, see Fig. 1a,b: the broad resonance at $\Delta_g \simeq 0$, the dark resonance (EIT) at $\Delta_g = \Delta_r$, and the narrow resonance at $\Delta_g = \Delta_r + \delta$, where

$$\delta = (\sqrt{\Delta_r^2 + \Omega_r^2} - |\Delta_r|) / 2 \quad (4)$$

is the ac-Stark shift created by the coupling laser.

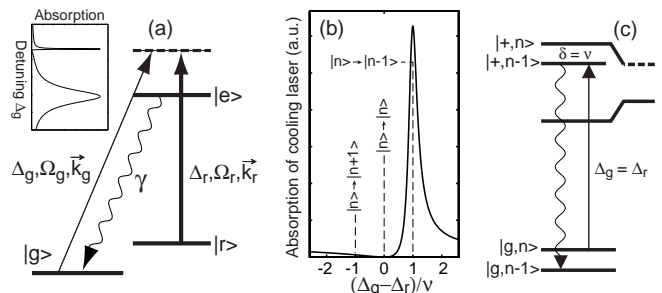


FIG. 2. (a) Levels and transitions of the EIT-cooling scheme. The inset shows schematically the absorption rate on $|g\rangle \rightarrow |e\rangle$ when the atom is strongly excited above resonance on $|r\rangle \rightarrow |e\rangle$. (b) Absorption of cooling laser around $\Delta_g = \Delta_r$ (solid line); probabilities of carrier ($|n\rangle \rightarrow |n\rangle$) and sideband ($|n\rangle \rightarrow |n \pm 1\rangle$) transitions when $\Delta_g = \Delta_r$ are marked by dashed lines. (c) Dressed state picture: the cooling laser excites resonantly transitions from $|g, n\rangle$ to the narrow dressed state denoted by $|+, n-1\rangle$ which preferentially decays into $|g, n-1\rangle$.

For EIT-cooling, the laser frequencies are set to the dark resonance condition, $\Delta_g = \Delta_r$. Then, taking into account the harmonic motion, all $|g, n\rangle \rightarrow |e, n\rangle$ transitions are cancelled. Furthermore, by choosing a suitable Rabi frequency Ω_r , the spectrum is designed such that the $|g, n\rangle \rightarrow |e, n-1\rangle$ (red) sideband corresponds to the maximum of the narrow resonance, whereas the blue sideband falls into the region of the spectrum of small excitation probability, as shown in Fig. 1b. The conditions for enhancing the red-sideband absorption while eliminating the carrier is therefore:

$$\Delta_g = \Delta_r \quad ; \quad \delta \simeq \nu \quad (5)$$

In summary, due to the EIT condition no absorption happens unless the ion is moving, and by adjusting the coupling Rabi frequency such that the bright resonance matches the red sideband, absorption accompanied by the loss of one phonon is made much more probable than absorption accompanied by gaining one phonon. The fact that the diffusion normally caused by $|n\rangle \rightarrow |n\rangle$ absorption is eliminated is most important for three-dimensional cooling, since the cooling limit $\langle n \rangle$ becomes independent of the projection of the vibrational mode on the laser direction [15].

C. Cooling dynamics

A calculation starting from the full quantum mechanical master equation [16] shows that in the Lamb-Dicke regime and below saturation of the cooling transition, the EIT-cooling process can be approximated by the same rate equation discussed above, only that now the appropriate coefficients A_{\pm} contain the quantum interference around $\Delta_{\pi} = \Delta_{\sigma}$. The explicit form of the coefficients is given in [15]. Fig. 3 shows the cooling dynamics calculated from a Monte-Carlo simulation of the master equation and from the rate equation approximation.

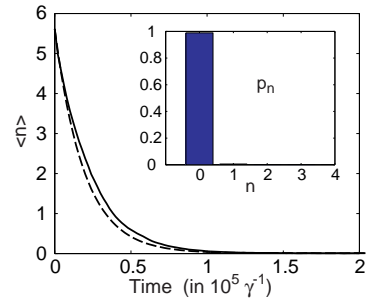


FIG. 3. Onset: $\langle n \rangle$ as a function of time calculated with full Monte Carlo simulation (solid line) and rate equation (dashed line). Parameters are $\Omega_r = \gamma$, $\Omega_g = \gamma/20$, $\nu = \gamma/10$, $\eta = 0.145$, $\Delta_g = \Delta_r = 2.5\gamma$. Inset: Steady state distribution p_n .

D. Example calculations

EIT-cooling shows to be a robust technique even if the system involved deviates from the ideal 3-level scheme. For example, in the experiments described below, due to non-ideal polarizations of the laser beams, photons were scattered from a fourth level which introduced extra heating. The theoretical cooling limit for this particular case increases by about a factor of 3, and the experiment still yielded cooling close the ground state [17], see Sec. III.

Another interesting situation is when the excited state decays through an additional channel into a fourth level from which it has to be repumped with an additional laser. We studied the example of a single trapped Hg^+ ion where the states $|g\rangle, |r\rangle, |e\rangle$ for EIT-cooling are taken to be the $S_{1/2}(F=1, m_F=1, 0)$ and $P_{1/2}(F=1, m_F=1)$ levels, respectively. The $S_{1/2}(F=0, m_F=0)$ level into which $|e\rangle$ decays with $1/3$ probability is pumped out resonantly back to $|e\rangle$. Our model calculation is shown in Fig. 4. A cooling limit of $\langle n \rangle \simeq 1$ is achieved which is significantly below the Doppler cooling limit of about 20 and which could help to improve the Hg^+ single ion frequency standard [18].

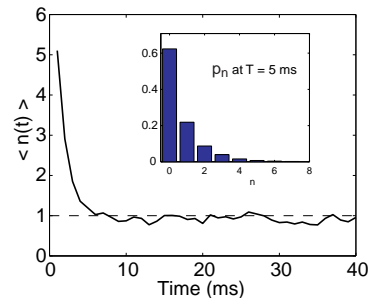


FIG. 4. Onset: $\langle n \rangle$ as a function of time calculated with full Monte Carlo simulation for a single trapped Hg^+ ion. Parameters are $\gamma = 64$ MHz, $\nu = 1.5$ MHz, $\Omega_r = 21$ MHz, $\Omega_g = 4$ MHz, $\Delta_r = \Delta_g = 80$ MHz, $\Omega_{repump} = 2$ MHz, $\Delta_{repump} = 0$. Inset: Steady state distribution p_n .

Finally, it would certainly be also interesting to apply EIT-cooling in cold-atom experiments, e.g. to Rb or Cs. In fact, the outer m -states of any $J \rightarrow J$ transition offer a suitable level systems for its implementation. Specifically, we give an estimate for the application of EIT-cooling to ^{87}Rb atoms in a CO_2 -laser standing wave dipole trap [19]. One main difference to an ion trap are that the trap frequency is generally lower and varies along the laser beam waist. We assumed a distribution of trap frequencies between 25 and 50 kHz, corresponding to the intensity variation over one Rayleigh length. We applied the rate equation model to the $(F = 1, m_F = 0, 1) - (F' = 1, m_F = 1)$ 3-level system and included resonant repumping from $F = 2$. The detailed parameters and the calculated results are displayed in Fig. 5. According to that estimate it should be possible to cool to $\langle n \rangle < 1$, much below the Doppler cooling limit, on a time scale of ms.

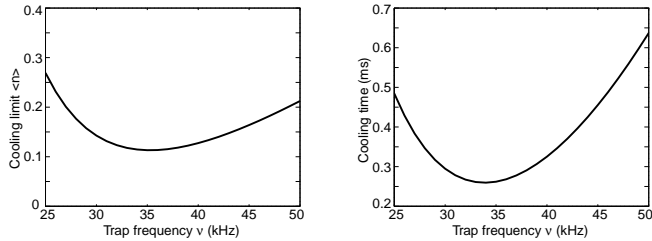


FIG. 5. Estimate for EIT-cooling of ^{87}Rb atoms in a CO_2 -laser standing wave trap: cooling limit (left) and cooling time (right) for trap frequencies of 25 .. 50 kHz. Parameters are $\gamma = 6$ MHz, $\Omega_r = 1.2$ MHz, $\Omega_g = 0.1$ MHz, $\Delta_r = \Delta_g = 10$ MHz, $\Omega_{repump} = 1$ MHz, $\Delta_{repump} = 0$.

It should be remarked that in this case the motional state before cooling may be outside the Lamb-Dicke regime, such that initially the considerations of Sec. II A do not apply. Instead, higher order sidebands, i.e. transitions with $|n - n'| > 1$ have to be taken into account. In the example of Fig. 5 one finds that the absorption probability for cooling transitions is larger than that for heating transitions for many higher-order sidebands (over several 100 kHz), therefore starting outside the Lamb-Dicke regime does not seem to restrict the application of EIT-cooling.

III. EIT-COOLING OF A SINGLE Ca^+ ION TO THE GROUND STATE

A. Levels and transitions in Ca^+

The theoretical background of the method described above has to be modified only slightly to apply it to our experiment with a single trapped Ca^+ ion. We implemented the EIT-scheme on the $S_{1/2} \rightarrow P_{1/2}$ transition, whose Zeeman sublevels $m = \pm 1/2$ constitute a four-level system. We denote these levels by $|S, \pm\rangle$ and $|P, \pm\rangle$, see Fig. 6. Three of the levels, $|S, \pm\rangle$ and $|P, +\rangle$, together with the σ^+ - and π -polarized laser beams, form an effective three-level system of the kind considered above [15]. The modifications due to the fourth level $|P, -\rangle$ are discussed in Sec. III E.

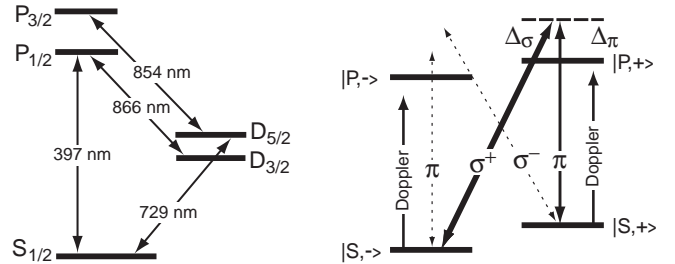


FIG. 6. Levels and transitions in $^{40}\text{Ca}^+$ used in the experiment (left side). The $S_{1/2}$ to $P_{1/2}$ transition is used for Doppler cooling and for EIT-cooling, and the scattered photons are observed to detect the ion's quantum state. The narrow $S_{1/2}$ to $D_{5/2}$ transition serves to investigate the vibrational state (see section III C). Shown on the right are the Zeeman sublevels of the $S_{1/2}$ and $P_{1/2}$ states (denoted by $|S, \pm\rangle$ and $|P, \pm\rangle$) and the laser frequencies relevant for cooling. The solid lines labeled by π and σ^+ are used for EIT-cooling, with $\Delta_\pi = \Delta_\sigma$. Dashed lines indicate further transitions which involve the $|P, -\rangle$ level.

B. Experimental setup

The Ca^+ system seems ideal for the demonstration of the EIT-cooling method since in previous experiments we have found very small heating rates [20] and therefore the cooling results can be measured with high precision. We will briefly introduce the experimental setup, for details we refer to [20,21]. First we describe all light sources which are necessary for the experiment:

For the $S_{1/2} \rightarrow P_{1/2}$ dipole transition at 397 nm, light from a Ti:Sapphire laser near 793 nm is frequency doubled in a LBO crystal inside a build-up cavity. Up to 5 mW of light near 397 nm are sent to the trap setup through a single mode UV fiber. As displayed in Fig. 7, we use the beam deflected into $+1^{st}$ order from an acousto-optical modulator (AO 1) driven at 80 MHz for Doppler cooling. Typically, this radiation is red-detuned from the resonance by 20 MHz. The two beams for EIT-cooling, labeled σ^+ and π , are derived from the

UV fiber output as the $+2^{nd}$ deflection orders of two further acousto-optical modulators AO 2 and AO 3 driven at 86 MHz and 92 MHz, respectively. We chose a detuning of $\Delta_\sigma = \Delta_\pi \simeq 75$ MHz (natural linewidth of the transition is 20 MHz). The difference in the AO 2 and 3 drive frequencies compensates for the 12 MHz Zeeman splitting of the $|S, \pm\rangle$ states in the quantization B-field of 4.4 Gauss. The three output beams are focused onto the single ion in the Paul trap from different directions corresponding to their respective polarisations and the orientation of the B-field. For a reproducible and fine tuning of the light intensity (typically few 10 μ W in a waist of $\simeq 60$ μ m) the rf-drive power of all AO's is computer-controlled. The rf-power, and therefore the light beams, can also be switched on and off within a few μ s.

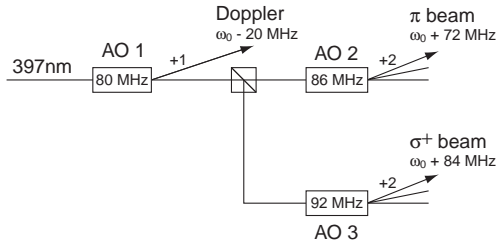


FIG. 7. Optical setup for the light beams at 397 nm. Inset: Scheme of the frequencies, as used for the Doppler- and for the EIT-cooling. Both EIT-beams are blue detuned. The Doppler cooling beam is red from Ca^+ ion resonances $|-, S\rangle \rightarrow |-, P\rangle$ and $|+, S\rangle \rightarrow |+, P\rangle$.

Light from a second Ti:Sapphire laser near 729 nm is used for excitation on the quadrupole transition from the $S_{1/2}$ ground state to the metastable $D_{5/2}$ state (spontaneous lifetime 1 s). The laser frequency is stabilized to a bandwidth of $\delta\nu \leq 100$ Hz using a stable high-finesse optical reference cavity and a Pound-Drever-Hall servo circuit. The laser frequency can be tuned by an acousto-optical modulator, its intensity is controlled through the rf-drive power. With this laser we can selectively excite vibrational sidebands of the $S_{1/2}-D_{5/2}$ transition at a few MHz detuning from the carrier. The relative excitation probability on the first red and the first blue sideband reveals information about the ion's vibrational quantum state as described in sect. III C.

The light of grating stabilized laser diodes near 866 nm and 854 nm serves to pump the ion out of both metastable D levels. While the light of the laser at 866 nm is turned on continuously throughout the experiment, the laser at 854 nm is also switched on and off by a computer-controlled acousto-optical modulator.

Our ion trap is a 3D-quadrupole Paul trap: A ring with inner diameter of 1.4 mm is formed from a Mb-wire of 0.2 mm diameter, and two endcaps are made out of sharpened tips of the same material at 1.2 mm distance [20]. The ring electrode is driven by $\simeq 650$ V ra-

dio frequency at 20.9 MHz, while the tips are held near ground potential. For the experiments described below, a single $^{40}\text{Ca}^+$ ion is generated by electron bombardment of a weak thermal Calcium beam. Its oscillation frequencies in the trap potential (ν_x, ν_y, ν_z) are (1.69, 1.62, 3.32) MHz. Additional compensation electrodes, together with a differential voltage applied to the tips, can be used to compensate for stray static electric fields and to shift the ion into the center of the rf-potential.

C. Measuring the vibrational quantum state

The average motional quantum number \bar{m} can be measured with high precision using laser excitation of vibrational sidebands, which are spectrally well resolved since the linewidth of the transition, here $S_{1/2}-D_{5/2}$, is well below the vibrational frequencies of the trapped ion. The situation is schematically depicted in Fig. 8, where the level scheme obtained for a two-level atom in a harmonic trapping potential is shown together with the carrier ($|n\rangle - |n\rangle$) and the first sideband ($|n\rangle - |n \pm 1\rangle$) transitions.

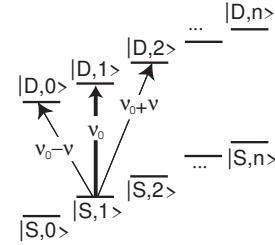


FIG. 8. Principle of temperature measurement. Transitions from $|S, n\rangle$ to $|D, n \pm 1\rangle$ are selectively laser-excited and the relative excitation probability is measured. ν_0 is the bare atomic transition frequency.

The excitation probabilities P_{red} and P_{blue} on the $|S, n\rangle$ to $|D, n - 1\rangle$ transition (red sideband) and the $|S, n\rangle$ to $|D, n + 1\rangle$ transition (blue sideband) are proportional to n and $n + 1$, respectively. P_{red} drops to zero for $|n = 0\rangle$, see Fig. 8. For a thermal phonon distribution with mean phonon number \bar{m} , the probability for finding n phonons is $p_n(\bar{m}) = \bar{m}^n / (\bar{m} + 1)^n$. Thus \bar{m} is directly related to the measured ratio $P_{red}/P_{blue} = \bar{m}/(\bar{m} + 1)$. It can be shown that this result holds for incoherent and coherent excitation if the phonon distribution $p_n(\bar{m})$ is thermal. Our cooling results will be specified either as \bar{m} or by the zero-phonon occupation p_0 for the three trap vibrational modes.

One way to determine the cooling result is to first excite a vibrational sideband at 729 nm and then probe the $S_{1/2}-P_{1/2}$ transition at 397 nm (shelving method) [6]. If sideband excitation to the $D_{5/2}$ state was successful, no fluorescence is emitted on the $S_{1/2}-D_{5/2}$ transition,

whereas in the other case we observe many scattered photons. This procedure is repeated 100 times on both the red and the blue sideband, and the difference in their excitation probabilities yields \bar{m} and p_0 .

The second method we used is driving coherent Rabi oscillations on the blue sideband [20,22]. We record the excitation probability $P_{blue}(t)$ as a function of 729 nm excitation time t . Theoretically, $P_{blue}(t) = \sum p_n(\bar{m}) \sin(\eta\Omega_{Rabi}\sqrt{n+1} t)$, where Ω_{Rabi} denotes the $S_{1/2}-D_{5/2}$ Rabi frequency and η the Lamb-Dicke factor [23]. The analysis of a time evolution $P_{blue}(t)$ reveals the mean phonon number \bar{m} or can even be used to measure all coefficients of the phonon distribution $p_n(\bar{m})$.

D. Setting the power level for the EIT-beams

Applying the EIT-cooling principle to our system, we find that the intensity of the EIT- σ^+ beam should be such that the Stark shift equals the frequency of the vibrational mode to be cooled. If the waist sizes of the beams are known, their intensities can be calculated. There are also a few possible methods to experimentally determine the ac-Stark shift or the corresponding Rabi frequencies:

- a) A rough estimate may be gained from the fluorescence rate as a function of light power. Finding first the approximate saturation power level, one can then deduce the necessary laser power for both EIT-beams.
- b) In the $\{S_{1/2}, P_{1/2}, D_{3/2}\}$ three-level system excited by the 866 nm and 397 nm lasers, one can measure the fluorescence rate if one of the laser frequencies is tuned over the resonance and the other is kept fix. Optical Bloch equations are then used to fit the excitation spectrum and determine the relevant Rabi frequencies [24].
- c) The time constant of optical pumping between the $|S, \pm\rangle$ states may be used. To probe their population, one of the two states must be selectively excited to the $D_{5/2}$ level.
- d) One can measure the broadening and ac-Stark shift of the narrow $S_{1/2}$ to $D_{5/2}$ transition when the ion is simultaneously illuminated with a pulse of 729 nm and one of the EIT-beams.

We used the last method to determine the ac-Stark shift δ as a function of power in the EIT-beams. From this, we could extrapolate to the power level where $\delta = \nu_{trap}$. In more detail, the ion was excited on the $S_{1/2}(m=1/2) \rightarrow D_{5/2}(m=5/2)$ transition with a 3 μ s pulse at 729 nm and *simultaneously* with a EIT- σ^+ pulse. Although the method suffered from asymmetric excitation line shapes and from rapid optical pumping out of the $S_{1/2}, m=1/2$ level, it lead to a good estimate for the right power level. For a final optimization of the EIT- σ^+ beam power we used the cooling results for a specific vibrational mode [17].

E. EIT-cooling experimental procedure

We investigated EIT cooling of the y and the z oscillation at 1.62 and 3.32 MHz, respectively. The experiment proceeded in three steps: Doppler precooling, EIT-cooling and finally determination of the vibrational quantum state, see Fig. 9:

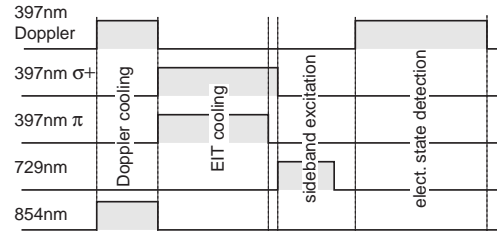


FIG. 9. Experimental pulse sequence. A 1.5 ms period of Doppler cooling is followed by a period of EIT-cooling (varied between 0 and 7.9 ms). The σ^+ -beam is left on 50 μ s longer than the π -beam to optically pump the ion into $|S, +\rangle$. The analysis of the vibrational state uses a pulse (of length t) at 729 nm for sideband excitation, followed by a Doppler pulse at 397 nm to probe the shelving. The laser at 866 nm continuously empties the $D_{3/2}$ level. The whole sequence of 20 ms duration is repeated 100 times for each sideband and the average excitation rate is calculated. To avoid 50 Hz magnetic field fluctuations the sequence is triggered by the electric power line.

(i) We Doppler precooled the ion on the $S_{1/2}$ to $P_{1/2}$ transition at 397 nm (natural linewidth $\Gamma \simeq 20$ MHz). A detuning of approximately -20 MHz with respect to the $S_{1/2} - P_{1/2}$ transition line was chosen. To avoid optical pumping into the $D_{3/2}$ states, we used the repumping beam near 866 nm [21]. Doppler cooling was applied for 1.5 ms. The theoretical Doppler cooling limit on this transition of 0.5 mK corresponds to mean vibrational quantum numbers of $\bar{m}^z \approx 3$ and $\bar{m}^x \approx \bar{m}^y \approx 6$. The cooling limits reached in our experiment were higher, due to the fact that the simple assumption of a two level system in the determination of the Doppler limit does not hold in our case and because the 12 MHz Zeeman splitting of the $S_{1/2}$ state does not permit optimum detuning for all transitions between the substates. We experimentally determined the mean excitation numbers after Doppler cooling to be $\bar{m}^z = 6.5(1.0)$ and $\bar{m}^y = 16(2)$.

(ii) After Doppler cooling, we applied the two EIT-beams, 397nm- σ^+ and 397nm- π for up to 7.9 ms. A 1.8 ms pulse duration was found to be sufficient, longer cooling time did not lower the mean phonon number (see Sec. IV B where we will discuss the cooling time). The power levels were set as discussed above in Sec. III D. For our setup with laser beam waists of $\simeq 50 \mu$ m, a laser power of $\leq 50 \mu$ W was used for the σ^+ -beam.

The k -vectors of the two EIT-cooling beams enclosed an angle of 125° and illuminated the ion in such a way that

their difference $\Delta\vec{k}$ had a component along all trap axes ($(\phi_x, \phi_y, \phi_z) = (66^\circ, 71^\circ, 31^\circ)$, where ϕ_i denotes the angle between $\Delta\vec{k}$ and the respective trap axis). As a result, *all* vibrational directions were cooled. Since the vacuum recipient did not allow for two orthogonal beams, we could not realize the ideal constellation of Fig. 6: While the σ^+ -beam was parallel to the quantization axis as desired, the π -beam was not orthogonal to it and therefore had a σ^- -component. The extra excitation due to this non-ideal constellation is indicated in Fig. 6 by a dashed line. It results in a slightly higher final mean phonon number. A detailed discussion is found in Ref. [17].

(iii) We analyzed the vibrational state after EIT-cooling by spectroscopy on the $S_{1/2} \rightarrow D_{5/2}$ quadrupole transition at 729 nm, as described in Sec. III C. Finally a diode laser at 854 nm served to repump the ion from the $D_{5/2}$ to the $S_{1/2}$ level.

IV. EIT-COOLING RESULTS

A. Cooling results for a single mode of vibration

With the ac-Stark shift δ set to the frequency of the radial y-mode, we monitored the vibrational state after EIT-cooling by exciting the blue sideband of the $|S, +\rangle \rightarrow D_{5/2}(m = +5/2)$ transition with a 729 nm pulse and then measuring the $|S, +\rangle$ level occupation as a function of the pulse length t [20,17]. The observed Rabi-oscillations were subsequently fitted to determine the mean vibrational occupation number \bar{m}^y [22], see Fig. 10. The lowest mean vibrational number $\bar{m}^y = 0.18$ observed corresponds to a 84% ground state probability. We repeated this experiment on the z-mode at 3.3 MHz after having increased the intensity of the σ^+ -beam to adjust δ . For this mode, a minimum mean vibrational number of $\bar{m}^z = 0.1$ was obtained, corresponding to a 90% ground state probability.

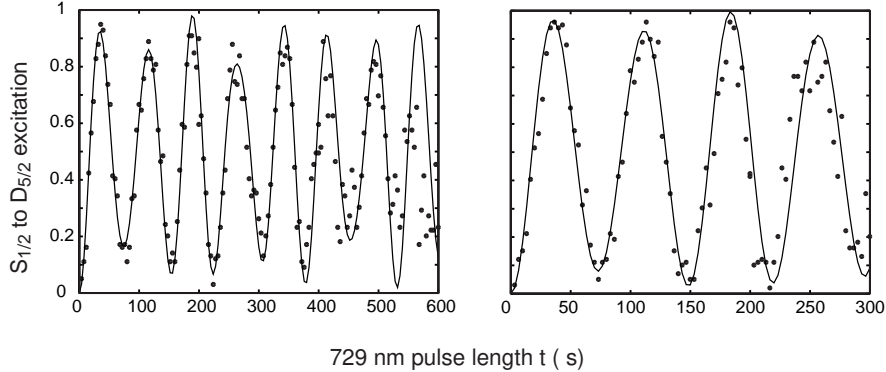


FIG. 10. Rabi oscillations excited on the blue sideband of the radial y-mode (left) and the axial z-mode (right) of a single ion. From the theoretical curves for $P_{blue}(\tau)$, mean phonon numbers of $\bar{m}^y = 0.18$ and $\bar{m}^z = 0.1$ are determined (see Sec. III C).

We found the cooling results largely independent of the intensity of the π -beam as long as it is much smaller than the σ^+ intensity. In our experiment the intensity ratio was $I_\sigma/I_\pi \simeq 100$ and we varied the intensity of the π -beam by a factor of 4, with no observable effect on the final \bar{m} .

B. Cooling dynamics

By determining the dependence of the mean vibrational quantum number on the EIT cooling time, we measured the cooling time constant for the y-mode to be $250 \mu s$, as shown in Fig. 11.

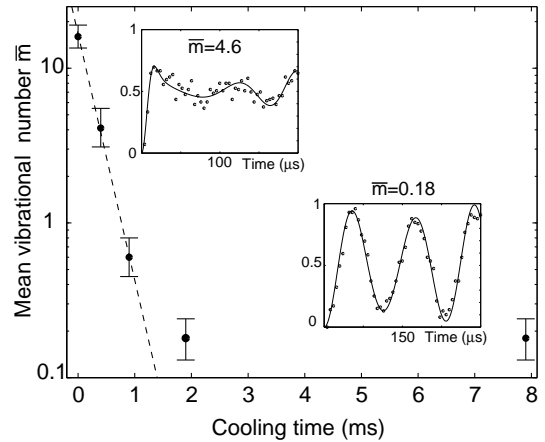


FIG. 11. Mean vibrational quantum number \bar{m}^y versus EIT cooling time. The insets show Rabi oscillations excited on the upper motional sideband of the $|S, +\rangle \rightarrow D_{5/2}(m = +5/2)$ transition, after 0.4 ms (left) and 7.9 ms (right) of EIT cooling. A thermal distribution is fitted to the data to determine \bar{m}^y in both cases.

C. Cooling of two modes

To show that the EIT method is suitable to simultaneously cool several vibrational modes with significantly different frequencies of oscillation, we chose the axial z -mode at 3.3 MHz, and the radial y -mode at 1.62 MHz. The intensity of the σ^+ -beam was set such that the ac-Stark shift was roughly halfway between the two mode frequencies. Again we applied the EIT cooling beams for 7.9 ms after Doppler cooling. This time we determined the final $\bar{m}^{y,z}$ by comparing the excitation probability on the red and the blue sidebands of the $S_{1/2}(m = 1/2) \rightarrow D_{5/2}(m = 5/2)$ transition. The result is shown in Fig. 12. We find both modes cooled deeply inside the Lamb-Dicke regime ($\eta\sqrt{\bar{m}} \simeq 0.02 \ll 1$), with $p_0^y = 58\%$ and $p_0^z = 74\%$ ground state probability.

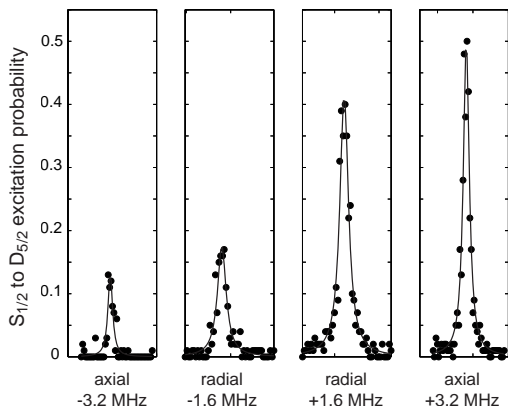


FIG. 12. EIT-cooling of two modes at 1.6 MHz and 3.2 MHz simultaneously. From the sideband excitation rate after cooling we deduce a ground state occupation number of 73% for the axial mode (3.2 MHz) and 58% for the radial mode (1.6 MHz).

V. EIT-COOLING OF LINEAR ION STRINGS

Since EIT-cooling allows simultaneous cooling of several modes at different frequencies, it seems to be particularly suited for ion strings in linear traps. The frequencies of the axial vibrational eigenmodes of a linear string have been calculated [25,26] and measured [27]. For a 10-ion string trapped in a linear trap with a center-of-mass axial frequency of 0.7 MHz, the closest inter-ion spacing is found to be $3.0 \mu\text{m}$ ($4.5 \mu\text{m}$ for $N=5$). The

axial vibration frequencies are 0.7 MHz, 1.22 MHz, .. 4.6 MHz. The radial trap frequencies in a linear trap must be made sufficiently high in order to prevent a transition from the linear configuration of N ions to a zig-zag configuration. It was estimated that this transition occurs at $\nu_{rad}/\nu_{ax} \sim 0.73N^{0.86}$, thus the radial trap frequency must exceed 3.7 MHz for 10 ions (2 MHz for $N=5$) [28]. Typically, the radial frequency is chosen higher. The linear ion trap experiment at Innsbruck uses $\nu_{rad} \geq 4$ MHz, the Be^+ experiments at NIST [29] have $\nu_{rad} \geq 20$ MHz. Apart from the purely axial modes there exist $2N$ radial modes. Their frequencies arrange in a band below ν_{rad} which overlaps with the axial mode frequencies.

We now estimate the performance of EIT-cooling for a 10-ion string. The result is displayed in Fig. 13: For a 10-ion string indeed *all* $3N$ vibrational modes are cooled to a mean phonon number \bar{m} below one. This is promising for the application of cold ion strings for quantum information processing [3–5,1]. As discussed in the introduction, it is required that all modes which couple to the laser light (spectator modes) must be cooled well into the Lamb-Dicke regime. The reason for that is that thermally excited spectator modes cause a blurring of the Rabi frequency Ω which disturbs the precision of quantum operations. For the case of $3N - 1$ spectator modes i with \bar{m}^i and Lamb-Dicke factors η_i , the initial state is a mixed state. Each time the experiment will happen with slightly different initial conditions and the Rabi frequency for carrier or sideband transitions will differ. The relative blurring reads like $\Delta\Omega/\Omega = \sqrt{\sum \eta_i^4 \bar{m}^i (\bar{m}^i + 1)/(3N - 1)}$ (see equ. 126 in ref. [28]) which we find as small as $3 \cdot 10^{-4}$ for our specific example. The maximum number of Rabi oscillations will then be $\sim (\Delta\Omega/\Omega)^{-1} \sim 2000$.

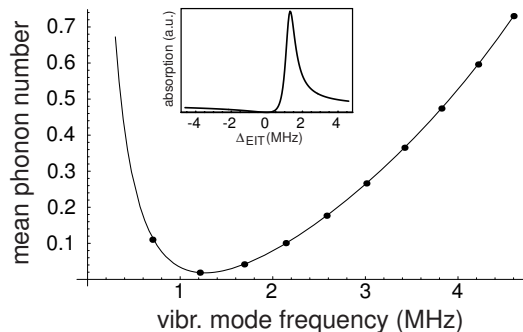


FIG. 13. EIT-cooling of the axial modes of a linear string based on the $S_{1/2} - P_{1/2}$ transition with $\Omega_\sigma = 30$ MHz, $\Omega_\pi = 0.5$ MHz, $\Gamma_P = 20$ MHz, and a detuning of $\Delta_\sigma = \Delta_\pi = 75$ MHz. The axial trap frequency is 0.7 MHz. For the calculation we have chosen the light intensity such that the bright state is ac-Stark shifted by ~ 3 MHz (see inset). The bright resonance with a width of ~ 0.5 MHz leads to cooling for all axial modes. The mean phonon numbers (black dots) of all axial modes are plotted versus the mode frequencies.

VI. CONCLUSION

In summary we have presented EIT-cooling, a novel ground state cooling method which uses electromagnetically induced transparency on two coupled dipole transitions. We have demonstrated its successful application to a single Ca^+ ion in a Paul trap. We have also shown several estimates for its implementation in various trapped-ion and trapped-atom experiments, taking into account different parameter regimes as well as deviations from the ideal case such as extra levels and transitions. The EIT-cooling method, according to these estimates and considering its experimental simplicity, bears the potential to become a standard tool for the preparation of ultracold atoms and ions. A particularly important application will be cooling of an ion string in a linear trap, as a step in preparing such a string for coherent manipulations in quantum information processing.

ACKNOWLEDGMENTS

This work is supported by the Austrian 'Fonds zur Förderung der wissenschaftlichen Forschung' (SFB15 and START-grant Y147-PHY), by the European Commission (TMR networks 'Quantum Information' (ERB-FRMX-CT96-0087) and 'Quantum Structures' (ERB-FMRX-CT96-0077)), and by the "Institut für Quanteninformatik GmbH".

⁺ Present address: Laboratoire Kastler-Brossel, Ecole Normale Supérieure, 24 rue Lhomond, 75005 Paris, France

^{*} Present address: NIST, 325 Broadway, Boulder, CO 80305, USA.

- [1] *The Physics of Quantum Information*. Springer, Berlin. ed. D. Bouwmeester, A. Ekert, and A. Zeilinger (2000).
- [2] H. C. Nägerl, D. Leibfried, H. Rohde, G. Thalhammer, J. Eschner, F. Schmidt-Kaler, R. Blatt, Phys. Rev. **A 60**, 145 (1999).
- [3] J. I. Cirac and P. Zoller, Phys. Rev. Lett. **74**, 4091 (1995).
- [4] K. Mølmer and A. Sørensen. Phys. Rev. Lett. **82**, 1835–1838 (1999)
- [5] K. Mølmer and A. Sørensen. Phys. Rev. **A 62**, 022311 (2000).
- [6] F. Diedrich, J. C. Bergquist, W. M. Itano, and D. J. Wineland, Phys. Rev. Lett. **62**, 403 (1989).
- [7] C. Monroe, D. M. Meekhof, B. E. King, S. R. Jefferts, W. M. Itano, and D. J. Wineland, Phys. Rev. Lett. **75**, 4011 (1995).
- [8] B. E. King, C. S. Wood, C. J. Myatt, Q. A. Turchette, D. Leibfried, W. M. Itano, C. Monroe, D. J. Wineland, Phys. Rev. Lett. **81**, 1525 (1998).
- [9] H. Rohde, S. T. Gulde, C. F. Roos, P. A. Barton, D. Leibfried, J. Eschner, F. Schmidt-Kaler, and R. Blatt, J. Opt. B: Quantum Semiclass. Opt. **3**, 34 (2001).
- [10] S. Stenholm, Rev. Mod. Phys. **58**, 699 (1986).
- [11] W. Neuhauser, M. Hohenstatt, P. Toschek, H. Dehmelt, Phys. Rev. Lett. **41**, 233 (1978).
- [12] α is between 1/5 and 2/5 depending on the type of transition and the orientation of quantization axis and vibration, $\alpha=1/3$ for isotropic emission, see also [10]
- [13] S. E. Harris, Phys. Today **50**, 36 (1997), and references therein.
- [14] B. Lounis and C. Cohen-Tannoudji, J. Phys. II (France) **2**, 579 (1992).
- [15] G. Morigi, J. Eschner and C. Keitel, Phys. Rev. Lett. **85**, 4458 (2000).
- [16] G. Morigi, unpublished.
- [17] C. F. Roos, D. Leibfried, A. Mundt, F. Schmidt-Kaler, J. Eschner, R. Blatt, Phys. Rev. Lett. **85**, 5547 (2000).
- [18] R. J. Rafac, B. C. Young, J. A. Beall, W. M. Itano, D. J. Wineland, and J. C. Bergquist, Phys. Rev. Lett. **85**, 2462 (2000).
- [19] R. Scheunemann, F. S. Cataliotti, T. W. Hänsch, and M. Weitz, Phys. Rev. **A 62**, 051801 (2000).
- [20] Ch. Roos, Th. Zeiger, H. Rohde, H.C. Nägerl, J. Eschner, D. Leibfried, F. Schmidt-Kaler, R. Blatt, Phys. Rev. Lett. **83**, 4713 (1999).
- [21] H. C. Nägerl, W. Bechter, J. Eschner, F. Schmidt-Kaler, and R. Blatt, Appl. Phys. B **66**, 603 (1998).
- [22] D. M. Meekhof, C. Monroe, B. E. King, W. M. Itano, and D. J. Wineland, Phys. Rev. Lett. **76**, 1796 (1996).
- [23] C. A. Blockley, D. F. Walls, and H. Risken, Europhys. Lett. **17**, 509 (1992); J. I. Cirac, R. Blatt, S. Parkins, and P. Zoller, Phys. Rev. A **49**, 1202 (1994).
- [24] G. Janik, W. Nagourney, H. Dehmelt, J. Opt. Soc. Am. B **2**, 1251 (1985); I. Siemers, M. Schubert, R. Blatt, W. Neuhauser, P. E. Toschek, Europhys. Lett. **18**, 139 (1992); M. Schubert, I. Siemers, R. Blatt, W. Neuhauser, P. E. Toschek, Phys. Rev. Lett. **68**, 3016 (1992); Phys. Rev. A **52**, 2994 (1995).
- [25] A. Steane. Appl. Phys. B **64**, 632 (1997).
- [26] D. V. F. James. Appl. Phys. B **66**, 181 (1998).
- [27] H. C. Nägerl, W. Bechter, J. Eschner, F. Schmidt-Kaler, and R. Blatt, Optics Express **3**, 89 (1998).
- [28] D. J. Wineland, C. Monroe, W. M. Itano, D. Leibfried, B. E. King, D. M. Meekhof, J. Res. Natl. Inst. Stand. Technol. **103**, 259 (1998).
- [29] Q. A. Turchette, D. Kielpinski, B. E. King, D. Leibfried, D.M. Meekhof, C. J. Myatt, M.A. Rove, C. A. Sackett, C. S. Wood, W. M. Itano, C. Monroe, and D. J. Wineland, Phys. Rev. **A 61**, 063418 (2000).